



# Numerical resolution of discontinuous Galerkin methods for time dependent wave equations <sup>☆</sup>

Xinghui Zhong, Chi-Wang Shu <sup>\*</sup>

Division of Applied Mathematics, Brown University, Providence, RI 02912, USA

## ARTICLE INFO

### Article history:

Received 9 December 2010

Received in revised form 30 April 2011

Accepted 17 May 2011

Available online 27 May 2011

### Keywords:

Discontinuous Galerkin method

Error analysis

Superconvergence

Fully discretized

Points per wavelength

## ABSTRACT

The discontinuous Galerkin (DG) method is known to provide good wave resolution properties, especially for long time simulation. In this paper, using Fourier analysis, we provide a quantitative error analysis for the semi-discrete DG method applied to time dependent linear convection equations with periodic boundary conditions. We apply the same technique to show that the error is of order  $k + 2$  superconvergent at Radau points on each element and of order  $2k + 1$  superconvergent at the downwind point of each element, when using piecewise polynomials of degree  $k$ . An analysis of the fully discretized approximation is also provided. We compute the number of points per wavelength required to obtain a fixed error for several fully discrete schemes. Numerical results are provided to verify our error analysis.

© 2011 Elsevier B.V. All rights reserved.

## 1. Introduction

In this paper, we consider the following time dependent linear wave problem

$$\begin{aligned} u_t + au_x &= 0, & x \in [0, 2\pi], & t > 0, \\ u(x, 0) &= e^{i\omega x}, & x \in [0, 2\pi], \end{aligned} \quad (1.1)$$

with periodic boundary conditions, where  $a$  is the phase speed (for simplicity, assume that  $a > 0$ ),  $i = \sqrt{-1}$  and  $\omega$  is the wave number (for convenience, assume that  $\omega > 0$ ). We develop a quantitative error analysis for the discontinuous Galerkin (DG) solution via Fourier analysis and study the superconvergence property of the DG solution. Because the Eq. (1.1) as well as the DG scheme are linear, a general  $L^2$  initial condition can be written as a sum of the simple waves  $e^{i\omega x}$  (Fourier series) and the numerical solution for such general initial condition is just a superposition of the numerical solution of the Eq. (1.1) with the simple wave initial condition. The results of this paper is therefore applicable to such general initial conditions when we have a clear objective to the wave numbers we would like to resolve. The quantitative analysis provided in this paper can be used in the application to guide the choice of mesh size and polynomial degree in the DG method, when we are solving

a linear wave equation, would like to resolve the first  $k$  waves, to a given threshold of error, up to a certain time  $t$ . The results of this paper is also valid for one dimensional linear hyperbolic system, and can provide useful guidelines when the DG method is used to solve more complicated linear and nonlinear wave equations.

DG methods are a class of finite element methods using completely discontinuous piecewise polynomials as basis functions. The first DG method was introduced by Reed and Hill [31] in 1973, to solve the neutron transport equation. The type of DG methods we will discuss in this paper is the Runge–Kutta discontinuous Galerkin (RKDG) method [22,21,19,18,23], which is using explicit and nonlinearly stable high order Runge–Kutta method for time discretization and the DG method for space discretization. This method has several advantages, such as local conservation, the allowance of arbitrary triangulation, excellent parallel efficiency, the capability in  $h$ - $p$  adaptivity and the ability to sharply capture discontinuities (especially contact discontinuities) in the solution. Furthermore, it has certain superconvergence properties.

The superconvergence behavior of the classical finite element method has been analyzed for many years. For example, in [25], Douglas and Dupont showed that for a general class of two-point boundary value problems, the rate of convergence at the mesh points is of order  $2k$  when polynomials of degree  $k$  are used. In [10], Bakker proved that the  $C^0$  Galerkin solution of a two-point boundary value problem using piecewise  $P^k$  polynomials, has superconvergence of order  $2k$  at the knots and of order  $k + 2$  at the Lobatto points of each segment, and the gradient is superconvergent of order  $k + 1$  at the zeros of a Legendre polynomial shifted to the elements of the partition. In [11], the same author proved

<sup>☆</sup> Research supported by NSF Grant DMS-0809086 and DOE Grant DE-FG02-08ER25863.

<sup>\*</sup> Corresponding author.

E-mail addresses: [xzhong@dam.brown.edu](mailto:xzhong@dam.brown.edu) (X. Zhong), [shu@dam.brown.edu](mailto:shu@dam.brown.edu) (C.-W. Shu).

that for two classes of Galerkin methods: the Ritz–Galerkin method for  $2m$ th order self-adjoint boundary value problems and the collocation method for arbitrary  $m$ th order boundary value problems, the solution has the superconvergence of order  $k + 2$  at the zeros of the Jacobi polynomial  $P_n^{m,m}(\sigma)$  shifted to the elements of the partition, and the derivative of the solution is superconvergent of order  $k + 1$  at the zeros of the Jacobi polynomial  $P_{n+1}^{m-1,m-1}(\sigma)$  shifted to the elements, where  $n = k + 1 - 2m$  and  $k$  is the degree of the finite element space.

Based on the results of Adjerid et al. [1] for singularly-perturbed parabolic systems, Biswas et al. [12] used the assumption that the DG solution of hyperbolic conservation laws using  $k$ -degree polynomial approximation exhibited superconvergence at the roots of Radau polynomial of degree  $k + 1$  (Radau points), to construct a posteriori estimate of spatial discretization error.

Adjerid et al. [2] proved that the DG solution of the ordinary differential equation (ODE)  $u' - f(u) = 0$  is superconvergent of order  $2k + 1$  at the downwind end of each element while maintaining an order of  $k + 2$  at the remaining Radau points. Numerical examples for the partial differential equations (PDEs) were also shown without analysis. Later, these results were extended to two-dimensional problems on rectangular meshes [4] and nonlinear hyperbolic problems [5]. Castillo [13] investigated the existence of superconvergent points for DG methods applied to elliptic problems and showed that on each element the  $k$ -degree local discontinuous Galerkin (LDG) solution gradient is superconvergent of order  $k + 1$  at the shifted roots of the  $k$ -degree Legendre polynomial. For these cases, the model problems are independent of time.

In [3], Adjerid and Klausner showed that the LDG solutions of convection-dominated problems are superconvergent of order  $k + 2$  at the shifted Radau points on each element. For diffusion-dominated problems, the derivative of the LDG solution is superconvergent of order  $k + 2$  at Radau points. Later, Adjerid et al. proved that the DG solution is superconvergent of order  $k + 2$  at Radau points for linear symmetric hyperbolic systems [6] and for linear symmetrizable hyperbolic systems [7], when  $t = O(1)$ . In this paper, by investigating the quantitative error at Radau points using Fourier analysis, we show that, even for  $t$  greater than  $O(1)$ , the errors at Radau points are of order  $k + 2$  with the exception of the Radau point at the downwind end of the element, which is of order  $2k + 1$ , when using DG method with piecewise polynomials of degree  $k$ . See, for example [29,14–17,20] for more superconvergence results of the DG method.

This work was motivated by [30], where the error analysis is given using the finite difference method. We first provide an overview of this method solving the linear wave problem (1.1). The exact solution of (1.1) is

$$U(x, t) = e^{i\omega(x-at)}.$$

Assume a uniform grid with  $\Delta x = \frac{2\pi}{N}$ , using the following second order central finite difference method to approximate the spatial derivative in (1.1)

$$D_0 u = \frac{u_{j+1} - u_{j-1}}{2\Delta x}$$

yields a semi-discrete version of (1.1) with a system of differential-difference equations given by

$$\frac{du_j(t)}{dt} + a \frac{u_{j+1}(t) - u_{j-1}(t)}{2\Delta x} = 0, \tag{1.2}$$

$$u_j(0) = e^{i\omega x_j}.$$

It is easy to compute the solution of (1.2), which is

$$u_j(t) = e^{i\omega(x_j-ct)},$$

with the numerical phase speed

$$c = \frac{a \sin \xi}{\xi}, \quad \xi = \omega \Delta x.$$

By Taylor expansion, the leading term in the error between the exact solution  $U(x, t)$  and the approximation solution  $u(x, t)$  is

$$e = \|U - u\|_\infty := \max_{0 \leq j \leq N} |U(x_j, t) - u_j(t)| \simeq \frac{\omega a t \xi^2}{6}. \tag{1.3}$$

It is evident that the error is a function of time. Under the assumption of periodicity, the important quantity is not the time elapsed, but rather the number of time periods, which is denoted by  $q$ , that is,

$$q = \frac{\bar{t}}{2\pi}, \quad \bar{t} = \omega a t. \tag{1.4}$$

Now the critical issue is: how many gridpoints are needed to resolve a wave, namely to make sure that the error is smaller than a given tolerance  $\varepsilon$ ? We introduce the number of points per wavelength,  $M$ , which is given by

$$M = \frac{N}{\omega} = \frac{2\pi}{\xi}. \tag{1.5}$$

Note that  $M$  has a theoretical minimum of 2, since it takes a minimum of two points per wavelength to uniquely specify a wave.

Rewriting the error (1.3) in terms of  $M$  and  $q$ , yields

$$e \simeq \frac{\pi q}{3} \left(\frac{2\pi}{M}\right)^2. \tag{1.6}$$

Then, the lower bound on  $M$

$$M \geq 2\pi \left(\frac{\pi}{3}\right)^{1/2} \left(\frac{q}{\varepsilon}\right)^{1/2},$$

required to ensure a specific error  $\varepsilon$  can be obtained from (1.6).

According to the analysis above, assume that we know for a given problem the maximum wave number  $\omega$  needed to adequately describe the solution. Then we can choose the number of points such that the wave is well resolved. This can reduce the cost of computation while preserving the accuracy. If more detailed information is known about the spectral distribution of the Fourier coefficients, then this can be used to obtain sharper comparisons of efficiency by weighting the error function appropriately.

In 1974, Swartz and Wendroff [33] extended the ideas of [30] to the finite element method, using smooth splines as basis functions and presented an analysis of fully discretized approximation. Our approach is to combine and extend the ideas of [30,33] to the DG method, using the techniques introduced in [35] (see also [34,36]) where the explicit formula of the DG solution is given by Fourier analysis. See, for example [32,27,28,8,9] for recent development and studies of the dispersion and dissipation errors of DG methods using Fourier analysis.

This paper is organized as follows: we first present the DG algorithm formulation for the model problem in Section 2. In Section 3, we present the details of the error analysis by Fourier analysis and provide the estimates of the necessary number of points per wavelength required to obtain a fixed error. In Section 4, we show that the DG solution is superconvergent at Radau points. In Section 5, an analysis of fully discretized approximation with Runge–Kutta methods as time discretization is presented. In Section 6, numerical experiments are provided to validate the results predicted by the analysis. Finally, concluding remarks are provided in Section 7.

## 2. Discontinuous Galerkin formulation

In this section, we present the algorithm formulation of the DG method solving the model problem

$$\begin{aligned} u_t + au_x &= 0, \quad x \in [0, 2\pi], t > 0, \\ u(x, 0) &= \sin \omega x, \quad x \in [0, 2\pi], \end{aligned} \tag{2.1}$$

with periodic boundary conditions. The exact solution to (2.1) is

$$U(x, t) = \sin(\omega(x - at)). \tag{2.2}$$

To define the DG method for the model problem, we consider a uniform partition of the computational domain  $[0, 2\pi]$  in  $N$  cells of size  $\Delta x = \frac{2\pi}{N}$ . Denote the cell by  $I_j = [x_{j-\frac{1}{2}}, x_{j+\frac{1}{2}}]$  and the cell center

$$\text{by } x_j = \frac{1}{2}(x_{j+\frac{1}{2}} + x_{j-\frac{1}{2}}), \quad j = 1, \dots, N, \text{ where}$$

$$0 = x_{\frac{1}{2}} < x_{\frac{3}{2}} < \dots < x_{N+\frac{1}{2}} = 2\pi$$

and denote the approximation space as

$$V_h^k = \left\{ v : v|_{I_j} \in P^k(I_j); 1 \leq j \leq N \right\}, \tag{2.3}$$

where  $P^k(I_j)$  denotes the set of polynomials of degree up to  $k$  defined on the cell  $I_j$ . The semi-discrete DG method using the upwind flux for solving (2.1) is defined as follows: find the unique function  $u = u(t) \in V_h^k$  such that, for  $j = 1, \dots, N$ ,

$$\int_{I_j} u_t v dx - a \int_{I_j} u v_x dx + a u_{j+\frac{1}{2}}^- v(x_{j+\frac{1}{2}}^-) - a u_{j-\frac{1}{2}}^- v(x_{j-\frac{1}{2}}^+) = 0 \tag{2.4}$$

holds for all test functions  $v \in V_h^k$ . Here and below  $u^+$ ,  $u^-$  denote the left and right limits of the function  $u$  at the cell interface, respectively.

We now look at the implementation of the scheme (2.4). If a local basis of  $P^k(I_j)$  is chosen and denoted as  $\phi_l^j(x)$  for  $l = 1, 2, \dots, k + 1$ , then the numerical solution can be represented as

$$u(x) = \sum_{l=1}^{k+1} u_j^l \phi_l^j(x), \quad x \in I_j. \tag{2.5}$$

After substituting (2.5) into (2.4) and inverting a local  $(k + 1) \times (k + 1)$  mass matrix, the DG scheme (2.4) can be written as

$$\frac{d\mathbf{u}_j}{dt} = \frac{a}{\Delta x} (\mathbf{A}\mathbf{u}_j + \mathbf{B}\mathbf{u}_{j-1}), \tag{2.6}$$

where  $\mathbf{u}_j = (u_j^1, \dots, u_j^{k+1})^T$ ,  $\mathbf{A}$  and  $\mathbf{B}$  are  $(k + 1) \times (k + 1)$  constant matrices.

As in [35], the local basis of  $P^k(I_j)$  is chosen to be the Lagrangian polynomials, based on the following  $k + 1$  equally spaced points

$$x_{j+\frac{2l-k}{2(k+1)}} = x_j + \left( \frac{2l-k}{2(k+1)} \right) \Delta x, \quad l = 0, \dots, k.$$

In this way,  $\mathbf{u}_j$ , the coefficients of the solution  $u$  inside the cell  $I_j$  is a vector of length  $k + 1$  containing the values of the solution at these points. The DG finite element scheme (2.6) becomes a finite difference scheme on a globally uniform mesh (with a mesh size  $\frac{\Delta x}{k+1}$ ). However, it is not a standard finite difference scheme because each point in the group of  $k + 1$  points belonging to the cell  $I_j$  obeys a different form.

### 3. Error analysis

In this section, we present the details of DG algorithm formulation with the basis functions discussed in Section 2 and derive the error estimation of the semi-discrete scheme using piecewise  $P^k$  polynomials, with  $k = 1, 2, 3$ . At the end of this section, We provide an estimate of the necessary number of points per wavelength required to obtain a fixed error.

#### 3.1. The case of $P^1$

In this subsection, we consider the piecewise linear case, i.e.  $k = 1$ . We present the details of the error analysis for this case.

In this case, the local basis functions inside cell  $I_j$  are  $\phi_{j-\frac{1}{4}}(x), \phi_{j+\frac{1}{4}}(x)$ , which are Lagrangian polynomials based on the

points  $x_{j-\frac{1}{4}}, x_{j+\frac{1}{4}}$ . With these basis functions, the solution inside the cell  $I_j$  is then represented by

$$u(x) = u_{j-\frac{1}{4}} \phi_{j-\frac{1}{4}}(x) + u_{j+\frac{1}{4}} \phi_{j+\frac{1}{4}}(x).$$

The finite difference representation of the DG method is

$$\begin{aligned} u'_{j-\frac{1}{4}} &= \frac{a}{4\Delta x} \left( -5u_{j-\frac{5}{4}} + 15u_{j-\frac{3}{4}} - 7u_{j-\frac{1}{4}} + 3u_{j+\frac{1}{4}} \right), \\ u'_{j+\frac{1}{4}} &= \frac{a}{4\Delta x} \left( u_{j-\frac{5}{4}} - 3u_{j-\frac{3}{4}} + 11u_{j-\frac{1}{4}} - 9u_{j+\frac{1}{4}} \right). \end{aligned} \tag{3.1}$$

The scheme (3.1) can be rewritten into the matrix form

$$\frac{d\mathbf{u}_j}{dt} = \frac{a}{\Delta x} (\mathbf{A}\mathbf{u}_j + \mathbf{B}\mathbf{u}_{j-1}), \tag{3.2}$$

where

$$\mathbf{u}_j = \begin{pmatrix} u_{j-\frac{1}{4}} \\ u_{j+\frac{1}{4}} \end{pmatrix}, \quad \mathbf{A} = \frac{1}{4} \begin{pmatrix} -7 & -3 \\ 11 & -9 \end{pmatrix}, \quad \mathbf{B} = \frac{1}{4} \begin{pmatrix} -5 & 15 \\ 1 & -3 \end{pmatrix}. \tag{3.3}$$

To solve (3.2), the standard Fourier analysis is used here. This analysis depends heavily on the assumption of uniform mesh and periodic boundary conditions. Assume

$$\begin{pmatrix} u_{j-\frac{1}{4}}(t) \\ u_{j+\frac{1}{4}}(t) \end{pmatrix} = \begin{pmatrix} \hat{u}_{-\frac{1}{4}}(t) \\ \hat{u}_{\frac{1}{4}}(t) \end{pmatrix} e^{i\omega x_j} \tag{3.4}$$

and after substituting (3.4) into the DG scheme (3.2), the coefficient vector satisfies the following ODE system

$$\begin{pmatrix} \hat{u}'_{-\frac{1}{4}}(t) \\ \hat{u}'_{\frac{1}{4}}(t) \end{pmatrix} = G \begin{pmatrix} \hat{u}_{-\frac{1}{4}}(t) \\ \hat{u}_{\frac{1}{4}}(t) \end{pmatrix}, \tag{3.5}$$

where  $G$  is the amplification matrix, given by

$$G = \frac{a}{\Delta x} (\mathbf{A} + \mathbf{B}e^{-i\xi}), \quad \xi = \omega\Delta x. \tag{3.6}$$

The two eigenvalues of  $G$  are

$$\lambda_{1,2} = \frac{a}{\Delta x} \left( -e^{-i\xi} - 2 \mp \sqrt{e^{-2i\xi} + 10e^{-i\xi} - 2} \right) \tag{3.7}$$

and the corresponding eigenvectors are

$$V_{1,2} = \begin{pmatrix} -1 + e^{i\xi} \mp 4\sqrt{1 + 10e^{i\xi} - 2e^{2i\xi}} \\ 1 + 11e^{i\xi} \end{pmatrix}. \tag{3.8}$$

Then the general solution of the ODE system (3.5) is

$$\begin{pmatrix} \hat{u}_{-\frac{1}{4}}(t) \\ \hat{u}_{\frac{1}{4}}(t) \end{pmatrix} = C_{11} e^{\lambda_1 t} V_1 + C_{12} e^{\lambda_2 t} V_2. \tag{3.9}$$

The coefficients  $C_{11}$  and  $C_{12}$  in (3.9) can be determined by the initial condition

$$\begin{pmatrix} \hat{u}_{-\frac{1}{4}}(0) \\ \hat{u}_{\frac{1}{4}}(0) \end{pmatrix} = \begin{pmatrix} e^{-\frac{i\xi}{4}} \\ e^{\frac{i\xi}{4}} \end{pmatrix}. \tag{3.10}$$

We thus have the explicit solution of the DG scheme with piecewise linear polynomials for solving (2.1). Comparing with the exact solution (2.2) will give us the quantitative error. Now let us first introduce some notations:

$$\begin{aligned} \|e_{-\frac{1}{4}}\|_\infty &:= \max_{1 \leq j \leq N} |U(x_{j-\frac{1}{4}}, t) - u_{j-\frac{1}{4}}(t)|, \\ \|e_{+\frac{1}{4}}\|_\infty &:= \max_{1 \leq j \leq N} |U(x_{j+\frac{1}{4}}, t) - u_{j+\frac{1}{4}}(t)|. \end{aligned} \tag{3.11}$$

By a simple Taylor expansion, we get

$$\begin{aligned} \|e_{+\frac{1}{4}}\|_\infty &= \frac{1}{24}\bar{t}^2 + \frac{\bar{t}}{72}\bar{t}^3 - \frac{211}{27648}\bar{t}^4 - \frac{1861\bar{t}}{414720}\bar{t}^5 \\ &+ \left(\frac{2808495 + 1364224\bar{t}}{1592524800}\right)\bar{t}^6 \\ &- \left(\frac{11(-2854295\bar{t} + 965888\bar{t}^2)}{33443020800}\right)\bar{t}^7 \\ &+ \left(\frac{-6386427605 + 581426944\bar{t}^2 + 1359970304\bar{t}^4}{12842119987200}\right)\bar{t}^8 \\ &- \left(\frac{48576117895\bar{t} - 7643182848\bar{t}^3 + 6799851520\bar{t}^5}{192631799808000}\right)\bar{t}^9 \\ &+ O(\bar{t}^{10}), \end{aligned} \tag{3.12}$$

where  $\bar{t} = \omega at$ .

From (3.12), for short time  $\bar{t}$ , the first term  $\frac{1}{24}\bar{t}^2$ , which is independent of  $\bar{t}$ , dominates. As  $\bar{t}$  increases to  $O(\frac{1}{\xi})$ , the second term  $\frac{\bar{t}}{72}\bar{t}^3$  begins to dominate. If  $\bar{t}$  continues increasing, another term with higher degree of  $\bar{t}$  as coefficient may dominate. This means, during different time intervals, the dominant terms are different. At  $\bar{t} = O(\frac{1}{\xi})$ , the error can be approximated by the first two terms, i.e.

$$\begin{aligned} \|e_{-\frac{1}{4}}\|_\infty &\simeq \left| \frac{1}{24}\bar{t}^2 - \frac{1}{72}\bar{t}\bar{t}^3 \right|, \\ \|e_{+\frac{1}{4}}\|_\infty &\simeq \frac{1}{24}\bar{t}^2 + \frac{1}{72}\bar{t}\bar{t}^3. \end{aligned} \tag{3.13}$$

Denote  $e_1 = \max\{\|e_{-\frac{1}{4}}\|_\infty, \|e_{+\frac{1}{4}}\|_\infty\}$ , where the subscript 1 is used here to indicate the case  $k = 1$ . Clearly, the error  $e_1$  satisfies

$$e_1 = \max\left\{\|e_{-\frac{1}{4}}\|_\infty, \|e_{+\frac{1}{4}}\|_\infty\right\} \simeq \frac{1}{24}\bar{t}^2 + \frac{1}{72}\bar{t}\bar{t}^3. \tag{3.14}$$

Similar to the finite difference case, we would like to rewrite the error in terms of the number of points per wavelength  $M_1$  and the number of time periods  $q = \frac{t}{2\pi}$ . Notice that two points  $\{x_{j-\frac{1}{4}}, x_{j+\frac{1}{4}}\}$  are used for each cell, therefore,

$$M_1 = \frac{2N}{\omega} = \frac{4\pi}{\xi}. \tag{3.15}$$

Substituting (3.15) and (1.4) into (3.14), we get

$$e_1 \simeq \frac{1}{24}\left(\frac{4\pi}{M_1}\right)^2 + \frac{\pi q}{36}\left(\frac{4\pi}{M_1}\right)^3. \tag{3.16}$$

Then the number of points per wavelength required to guarantee the error  $e_1 \leq \varepsilon$  satisfies the following inequality

$$\frac{1}{24}\left(\frac{4\pi}{M_1}\right)^2 + \frac{\pi q}{36}\left(\frac{4\pi}{M_1}\right)^3 \leq \varepsilon. \tag{3.17}$$

### 3.2. The case of $P^2$

In this subsection, we use the same procedure as we did in the piecewise linear case to present the details of the error estimation of the DG method using piecewise  $P^2$  polynomials.

In this case, the local basis functions  $\{\phi_{j-\frac{1}{3}}(x), \phi_j(x), \phi_{j+\frac{1}{3}}(x)\}$  inside cell  $I_j$  are the Lagrangian polynomials based on the points  $x_{j-\frac{1}{3}}, x_j, x_{j+\frac{1}{3}}$ . The solution inside the cell  $I_j$  is then represented by

$$(x) = u_{j-\frac{1}{3}}\phi_{j-\frac{1}{3}}(x) + u_j\phi_j(x) + u_{j+\frac{1}{3}}\phi_{j+\frac{1}{3}}(x)$$

and the DG scheme can be written into the matrix form (2.6) with

$$u_j = \begin{pmatrix} u_{j-\frac{1}{3}} \\ u_j \\ u_{j+\frac{1}{3}} \end{pmatrix}, \quad A = \begin{pmatrix} -\frac{43}{16} & -\frac{29}{24} & \frac{1}{16} \\ \frac{69}{16} & -\frac{15}{8} & -\frac{15}{16} \\ -\frac{19}{16} & \frac{139}{24} & -\frac{71}{16} \end{pmatrix}, \quad B = \begin{pmatrix} \frac{23}{16} & -\frac{115}{24} & \frac{115}{16} \\ -\frac{9}{16} & \frac{15}{8} & -\frac{45}{16} \\ -\frac{1}{16} & \frac{5}{24} & -\frac{5}{16} \end{pmatrix}. \tag{3.18}$$

The standard Fourier analysis is again used here. First we make an ansatz of the form

$$\begin{pmatrix} u_{j-\frac{1}{3}}(t) \\ u_j(t) \\ u_{j+\frac{1}{3}}(t) \end{pmatrix} = \begin{pmatrix} \hat{u}_{-\frac{1}{3}}(t) \\ \hat{u}_0(t) \\ \hat{u}_{\frac{1}{3}}(t) \end{pmatrix} e^{i\omega x_j}. \tag{3.19}$$

After substituting (3.19) into the DG scheme (2.6) with (3.18), the coefficient vector satisfies

$$\begin{pmatrix} \hat{u}'_{-\frac{1}{3}}(t) \\ \hat{u}'_0(t) \\ \hat{u}'_{\frac{1}{3}}(t) \end{pmatrix} = G \begin{pmatrix} \hat{u}_{-\frac{1}{3}}(t) \\ \hat{u}_0(t) \\ \hat{u}_{\frac{1}{3}}(t) \end{pmatrix}, \tag{3.20}$$

where  $G$  is given by (3.6) with  $A$  and  $B$  defined in (3.18). Then with three eigenvalues of  $G$  and the corresponding eigenvectors computed by Mathematica, the general solution of the ODE system (3.20) is

$$\begin{pmatrix} \hat{u}_{-\frac{1}{3}}(t) \\ \hat{u}_0(t) \\ \hat{u}_{\frac{1}{3}}(t) \end{pmatrix} = C_{21}e^{\lambda_1 t}V_1 + C_{22}e^{\lambda_2 t}V_2 + C_{23}e^{\lambda_3 t}V_3. \tag{3.21}$$

The coefficients  $C_{21}$ ,  $C_{22}$  and  $C_{23}$  in (3.21) can be determined by the initial condition

$$\begin{pmatrix} \hat{u}_{-\frac{1}{3}}(0) \\ \hat{u}_0(0) \\ \hat{u}_{\frac{1}{3}}(0) \end{pmatrix} = \begin{pmatrix} e^{-\frac{ik}{3}} \\ 1 \\ e^{\frac{ik}{3}} \end{pmatrix}. \tag{3.22}$$

We thus have the explicit solution of the DG scheme with  $P^2$  polynomials for solving (2.1). Comparing with the exact solution (2.2) will give us the quantitative error estimates.

$$\begin{aligned} \|e_{-\frac{1}{3}}\|_\infty &:= \max_{1 \leq j \leq N} |U(x_{j-\frac{1}{3}}, t) - u_{j-\frac{1}{3}}(t)| \\ &= \frac{\xi^3}{1296} + \frac{3223\xi^5}{3110400} - \frac{241\bar{t}\xi^6}{1008000} \\ &+ \left(-\frac{110175241}{134369280000} + \frac{\bar{t}^2}{80000}\right)\xi^7 + O(\xi^8), \end{aligned}$$

$$\begin{aligned} \|e_0\|_\infty &:= \max_{1 \leq j \leq N} |U(x_j, t) - u_j(t)| \\ &= \frac{\xi^3}{240} - \frac{4979\xi^5}{15552000} - \frac{11\bar{t}\xi^6}{1814400} \\ &+ \left(\frac{28245223}{201553920000} + \frac{\bar{t}^2}{432000}\right)\xi^7 + O(\xi^8), \end{aligned}$$

$$\begin{aligned} \|e_{+\frac{1}{3}}\|_\infty &:= \max_{1 \leq j \leq N} |U(x_{j+\frac{1}{3}}, t) - u_{j+\frac{1}{3}}(t)| \\ &= \frac{23\xi^3}{6480} + \frac{67567\xi^5}{357696000} + \frac{263\bar{t}\xi^6}{4636800} \\ &- \left(\frac{451421052697}{8174355148800000} - \frac{\bar{t}^2}{368000}\right)\xi^7 + O(\xi^8). \end{aligned}$$

Clearly, the coefficients of high order terms depend on  $\bar{t}$ . Similarly, during different time intervals, the dominant terms are different.

Denote  $e_2 := \max \{ \|e_{-\frac{1}{3}}\|_\infty, \|e_0\|_\infty, \|e_{+\frac{1}{3}}\|_\infty \}$ . At  $\bar{t} = O(\frac{1}{\xi})$ , the error  $e_2$  satisfies

$$e_2 \simeq \frac{\xi^3}{240}. \tag{3.23}$$

At  $\bar{t} = O(\frac{1}{\xi^2})$ , the error  $e_2$  satisfies

$$e_2 \simeq \frac{\xi^3}{240} - \frac{4979\xi^5}{15552000} - \frac{11\bar{t}\xi^6}{1814400} + \left( \frac{28245223}{201553920000} + \frac{\bar{t}^2}{432000} \right) \xi^7. \tag{3.24}$$

In this case, the number of points per wavelength  $M_2$  satisfies

$$M_2 = \frac{3N}{\omega} = \frac{6\pi}{\xi}, \tag{3.25}$$

since three points are used in each cell. Similarly, by rewriting (3.23) and (3.24) in terms of  $M_2$  and  $q = \frac{\bar{t}}{2\pi}$ , we can obtain the number of points per wavelength  $M_2$  required to ensure that  $e_2 \leq \varepsilon$ .

3.3. The case of  $P^3$

In this subsection, we apply the same procedure discussed in the previous subsections to the DG method using piecewise  $P^3$  polynomials.

The local basis functions  $\{ \phi_{j-\frac{3}{8}}(x), \phi_{j-\frac{1}{8}}(x), \phi_{j+\frac{1}{8}}(x), \phi_{j+\frac{3}{8}}(x) \}$  inside cell  $I_j$  are the Lagrangian polynomials based on the points  $x_{j-\frac{3}{8}}, x_{j-\frac{1}{8}}, x_{j+\frac{1}{8}}, x_{j+\frac{3}{8}}$ . With these basis functions, the DG scheme can be written into the matrix form (2.6) with

$$A = \begin{pmatrix} -\frac{15109}{6144} & -\frac{4521}{2048} & \frac{255}{2048} & \frac{403}{6144} \\ \frac{43577}{6144} & -\frac{7699}{2048} & -\frac{1115}{2048} & -\frac{959}{6144} \\ -\frac{11761}{6144} & \frac{10747}{2048} & -\frac{5629}{2048} & -\frac{7097}{6144} \\ -\frac{4723}{6144} & -\frac{7983}{2048} & \frac{21993}{2048} & -\frac{43211}{6144} \end{pmatrix}$$

and

$$B = \begin{pmatrix} -\frac{2865}{2048} & \frac{12033}{2048} & -\frac{20055}{2048} & \frac{20055}{2048} \\ \frac{1685}{2048} & -\frac{7077}{2048} & \frac{11795}{2048} & -\frac{11795}{2048} \\ -\frac{365}{2048} & \frac{1533}{2048} & -\frac{2555}{2048} & \frac{2555}{2048} \\ -\frac{615}{2048} & \frac{2583}{2048} & -\frac{4305}{2048} & \frac{4305}{2048} \end{pmatrix}.$$

The standard Fourier analysis is once again used here to obtain the explicit solution of the DG scheme. The error is also approximated by the dominant terms of Taylor series. Denote

$$e_3 := \max \{ \|e_{-\frac{3}{8}}\|_\infty, \|e_{-\frac{1}{8}}\|_\infty, \|e_{+\frac{1}{8}}\|_\infty, \|e_{+\frac{3}{8}}\|_\infty \}. \text{ At } \bar{t} = O(\frac{1}{\xi^2}), \tag{3.26}$$

$$e_3 \simeq 0.00036369202628968253968253968254 \xi^4.$$

$$\text{At } \bar{t} = O(\frac{1}{\xi^3}),$$

$$e_3 \simeq 0.00036369202628968253968253968254 \xi^4$$

$$- 7.25319954423243464358961570099621 \times 10^{-6} \xi^6$$

$$+ 7.08616780045351473922902494331066 \times 10^{-7} \bar{t} \xi^7. \tag{3.27}$$

In this case, the number of points per wavelength  $M_3$  satisfies

$$M_3 = \frac{4N}{\omega} = \frac{8\pi}{\xi}, \tag{3.28}$$

since four points are used in each cell. Similarly, the number of points per wavelength  $M_3$  required to ensure that  $e_3 \leq \varepsilon$  can be obtained by rewriting (3.26) and (3.27) in terms of  $M_3$  and  $q$ .

Table 3.1 shows the lower bound of  $M_k$  to ensure the specific error  $\varepsilon$ , which is a function of  $q$  we only present the leading term here.

**Table 3.1**  
Leading term of the lower bound of  $M_k$  as a function of  $q$ .

$\bar{t}$	$M_2$		$M_3$	
	$O(\frac{1}{\bar{t}})$	$O(\frac{1}{\bar{t}})$	$O(\frac{1}{\bar{t}})$	$O(\frac{1}{\bar{t}})$
$\varepsilon = 0.1$	$12q^3$	6.53	$7q^3$	6.17
$\varepsilon = 0.01$	$26q^3$	14.08	$10q^3$	10.98
$\varepsilon = 0.001$	$56q^3$	30.33	$13q^3$	19.52

4. Superconvergence

In this section, we study the superconvergence property of the DG solution at Radau points.

4.1. Superconvergence at Radau points

In this subsection, we study the superconvergence property of DG solutions at Radau points. The local basis functions of  $P^k(I_j)$  are chosen to be the Lagrangian polynomials, based on the following  $k + 1$  points

$$x_{j+r_l} = x_j + \frac{\zeta_{k,l}}{2} \Delta x, \quad l = 0, \dots, k,$$

where  $\{\zeta_{k,l}\}$  are the roots of the Radau polynomial  $P_{k+1}(x) - P_k(x)$  and  $P_k(x)$  is the Legendre polynomial of degree  $k$ . Table 4.1 displays  $\{\zeta_{k,l}\}$  for  $k = 1, 2, 3$ . Note that  $x_{j+r_k} = x_{j+\frac{1}{2}}$  is the downwind point of the element  $I_j$ .

**Remark.** The basis functions in this section are different from those discussed in Section 3 and the amplification matrices are different, but they have the same eigenvalues. These eigenvalues are also the same with the ones derived in [32] using an orthonormal basis of Legendre polynomials.

As in Section 2, the DG method with the above basis can be written into a matrix form. The standard Fourier analysis is used to find the explicit solution of the DG scheme as discussed in Section 3. We do not repeat the details of this analysis procedure. Denote

$$\|e_{r_l}\|_\infty := \max_{1 \leq j \leq N} |U(x_{j+r_l}, t) - u(x_{j+r_l}, t)|,$$

$$\|e_{+\frac{1}{2}}^-\|_\infty := \max_{1 \leq j \leq N} |U(x_{j+\frac{1}{2}}^-, t) - u(x_{j+\frac{1}{2}}^-, t)|.$$

The followings are the error estimate results.

- $k = 1$

$$\|e_{r_0}\|_\infty = \frac{1}{72} \sqrt{\frac{16}{81} + \bar{t}^2 \xi^3} + O(\xi^4),$$

$$\|e_{+\frac{1}{2}}^-\|_\infty = \frac{1}{72} \sqrt{\frac{16}{9} + \bar{t}^2 \xi^3} + O(\xi^4);$$

**Table 4.1**  
 $\{\zeta_{k,l}\}_{l=0}^k$ : the roots of  $P_{k+1}(x) - P_k(x)$ .

	$\zeta_{k,l}$
$k = 1$	$\zeta_{1,0} = -\frac{1}{3}, \zeta_{1,1} = 1$
$k = 2$	$\zeta_{2,0} = -\frac{1+\sqrt{6}}{5}, \zeta_{2,1} = -\frac{1-\sqrt{6}}{5}, \zeta_{2,2} = 1$
$k = 3$	$\zeta_{3,0} = -0.82282408097459210520890771246109$ $\zeta_{3,1} = -0.18106627111853057827014749586234$ $\zeta_{3,2} = 0.57531892352169411205048377975200$ $\zeta_{3,3} = 1$

•  $k = 2$

$$\|e_{r_0}\|_\infty = \left| 0.00112979589711327123927891362988 \zeta^4 - \frac{\bar{t}}{7200} \zeta^5 \right| + O(\zeta^6),$$

$$\|e_{r_1}\|_\infty = 0.00082979589711327123927891362988 \zeta^4 + \frac{\bar{t}}{7200} \zeta^5 + O(\zeta^6),$$

$$\|e_{+\frac{1}{2}}^-\|_\infty = \frac{\sqrt{\bar{t}^2 + 144/25}}{7200} \zeta^5 + O(\zeta^6);$$

•  $k = 3$

$$\|e_{r_0}\|_\infty = \left| 4.58526548614820367915101051257673 \times 10^{-5} \zeta^5 + 1.48442413127661313280202433713330 \times 10^{-6} \zeta^7 - 2.95523546192529651029864723686194 \times 10^{-7} \bar{t} \zeta^8 \right| + O(\zeta^9),$$

$$\|e_{r_1}\|_\infty = 4.81347804829324175268316712031863 \times 10^{-5} \zeta^5 - 1.74662334589086702133200039227532 \times 10^{-6} \zeta^7 + 1.12983256993051227300311527010632 \times 10^{-8} \bar{t} \zeta^8 + O(\zeta^9),$$

$$\|e_{r_2}\|_\infty = 2.60817329279298238245105944584508 \times 10^{-5} \zeta^5 + 1.86838652276109018545310450926279 \times 10^{-6} \zeta^7 + 3.23693699988152665996155459585616 \times 10^{-7} \bar{t} \zeta^8 + O(\zeta^9),$$

$$\|e_{+\frac{1}{2}}^-\|_\infty = \frac{\sqrt{\bar{t}^2 + 576/49}}{1412200} \zeta^7 + \frac{3.207918913795226905503036041469 \times 10^{-7} \bar{t}}{\sqrt{576 + 49\bar{t}^2}} \zeta^8 + O(\zeta^9).$$

#### 4.2. Superconvergence at the downwind point

In this subsection, we take a particular look at the error at the downwind point of each cell.

Let  $M_k^f$  be the number of points per wavelength needed to guarantee the error  $\|e_{+\frac{1}{2}}^-\|_\infty \leq \varepsilon$  when using  $P^k$  polynomials. According to the results derived in the previous subsection, when  $\bar{t}$  is greater than  $O(1)$ , we have.

•  $k = 1$

$$\|e_{+\frac{1}{2}}^-\|_\infty = \frac{1}{72} \sqrt{\frac{16}{9} + \bar{t}^2} \zeta^3 + O(\zeta^4) \simeq \frac{\bar{t}}{72} \zeta = \frac{\pi q}{36} \left( \frac{4\pi}{M_1^f} \right)^3 \leq \varepsilon. \tag{4.1}$$

•  $k = 2$

$$\|e_{+\frac{1}{2}}^-\|_\infty = \frac{\sqrt{\bar{t}^2 + 144/25}}{7200} \zeta^5 + O(\zeta^6) \simeq \frac{\bar{t}}{7200} \zeta^5 = \frac{\pi q}{3600} \left( \frac{6\pi}{M_2^f} \right)^5 \leq \varepsilon. \tag{4.2}$$

•  $k = 3$

$$\|e_{+\frac{1}{2}}^-\|_\infty = \frac{\sqrt{\bar{t}^2 + 576/49}}{1412200} \zeta^7 + O(\zeta^8) \simeq \frac{\bar{t}}{1411200} \zeta^7 = \frac{\pi q}{705600} \left( \frac{8\pi}{M_3^f} \right)^7 \leq \varepsilon. \tag{4.3}$$

Therefore,

$$M_1^f \geq 4\pi \left( \frac{\pi}{36} \right)^{\frac{1}{3}} \left( \frac{q}{\varepsilon} \right)^{\frac{1}{3}}, \tag{4.4}$$

$$M_2^f \geq 6\pi \left( \frac{\pi}{3600} \right)^{\frac{1}{5}} \left( \frac{q}{\varepsilon} \right)^{\frac{1}{5}}, \tag{4.5}$$

$$M_3^f \geq 8\pi \left( \frac{\pi}{705600} \right)^{\frac{1}{7}} \left( \frac{q}{\varepsilon} \right)^{\frac{1}{7}}. \tag{4.6}$$

Table 4.2 shows the lower bound of  $M_k^f$  as a function of  $q$  for three representative values of  $\varepsilon$ , when  $\bar{t}$  is greater than  $O(1)$ .

### 5. Fully discrete schemes

The previous sections deal with the semi-discrete schemes. In practice, the time discretization also plays an important role. An analysis of fully discretized approximation will be presented in this section with the basis functions discussed in Section 3.

#### 5.1. The case of $P^1$

In this subsection, we present the details of fully discretized error analysis for the piecewise linear case.

Let  $\tilde{u}$  be the approximation solution of the differential-difference Eq. (2.4) obtained by using  $p$ -stage explicit Runge–Kutta methods of order  $p$  (RK  $(p, p)$ ) [26]. Then

$$\begin{pmatrix} \tilde{u}_{j-\frac{1}{4}} \\ \tilde{u}_{j+\frac{1}{4}} \end{pmatrix} = R^n \begin{pmatrix} e^{i\omega x_{j-\frac{1}{4}}} \\ e^{i\omega x_{j+\frac{1}{4}}} \end{pmatrix}, \quad n = \frac{t}{\Delta t}, \tag{5.1}$$

where

$$R = 1 + \Delta t G + \frac{\Delta t^2}{2!} G^2 + \dots + \frac{\Delta t^p}{p!} G^p, \tag{5.2}$$

with the amplification matrix  $G$  defined in (3.6). Let  $Q = [V_1, V_2]$  be the matrix with  $G$ 's eigenvectors as columns. Clearly, we have

$$Q^{-1} G Q = A = \begin{pmatrix} \lambda_1 & 0 \\ 0 & \lambda_2 \end{pmatrix}. \tag{5.3}$$

Denote  $\tilde{R} = Q^{-1} R Q$ . From (5.3) and (5.2), we have

$$\begin{aligned} \tilde{R} &= Q^{-1} R Q = 1 + \Delta t A + \dots + \frac{\Delta t^p}{p!} A^p \\ &= \begin{pmatrix} 1 + \Delta t \lambda_1 + \dots + \frac{\Delta t^p}{p!} \lambda_1^p & 0 \\ 0 & 1 + \Delta t \lambda_2 + \dots + \frac{\Delta t^p}{p!} \lambda_2^p \end{pmatrix}. \end{aligned}$$

Thus,

$$\begin{aligned} R^n &= (Q \tilde{R} Q^{-1})^n = Q \tilde{R}^n Q^{-1} \\ &= Q \begin{pmatrix} 1 + \Delta t \lambda_1 + \dots + \frac{\Delta t^p}{p!} \lambda_1^p & 0 \\ 0 & 1 + \Delta t \lambda_2 + \dots + \frac{\Delta t^p}{p!} \lambda_2^p \end{pmatrix}^n Q^{-1}. \end{aligned} \tag{5.4}$$

**Table 4.2**  
Lower bound of  $M_k^f$  as a function of  $q$ .

	$M_1^f$	$M_2^f$	$M_3^f$
$\varepsilon = 0.1$	$12q^{\frac{1}{3}}$	$7q^{\frac{1}{5}}$	$6q^{\frac{1}{7}}$
$\varepsilon = 0.01$	$25q^{\frac{1}{3}}$	$11q^{\frac{1}{5}}$	$8q^{\frac{1}{7}}$
$\varepsilon = 0.001$	$55q^{\frac{1}{3}}$	$18q^{\frac{1}{5}}$	$11q^{\frac{1}{7}}$

Substituting (5.4) into (5.1), we can determine the explicit solution of the RKDG scheme for solving (2.1). Comparing with the exact solution (2.2) will give us the quantitative error estimates, based on the assumption  $cfl = a \frac{\Delta t}{\Delta x}$ .

By a simple Taylor expansion, the error between the DG solution with RK (2,2) time discretization and the exact solution is

$$\begin{aligned} \tilde{u}_{j-\frac{1}{4}} - U(x_{j-\frac{1}{4}}, t) &= \frac{\xi^2}{24} (1 - 4icfl^2 \bar{t}) e^{-i\bar{t}} \\ &\quad - \frac{\xi^2}{24} (1 - 6cfl + 18cfl^2) \frac{\Delta t}{cfl \Delta x} e^{-\frac{3i(-1+6cfl)\bar{t}}{1-6cfl+18cfl^2}} \\ &\quad + \frac{\xi^3}{576} (-i - 8\bar{t} - 24cfl^2 + 72cfl^3 \bar{t}) e^{-i\bar{t}} \\ &\quad + \frac{\xi^3}{576} i (1 - 6cfl + 18cfl^2) \frac{\Delta t}{cfl \Delta x} e^{-\frac{3i(-1+6cfl)\bar{t}}{1-6cfl+18cfl^2}} \\ &\quad + \frac{\xi^3}{24} \bar{t} (1 - 6cfl + 18cfl^2) \frac{\Delta t}{cfl \Delta x} e^{-\frac{3i(-1+6cfl)\bar{t}}{1-6cfl+18cfl^2}} + \dots \end{aligned}$$

where  $\xi = \omega \Delta x$  and  $\bar{t} = \omega t$ .

In order to let the terms with coefficients  $(1 - 6cfl + 18cfl^2) \frac{\Delta t}{cfl \Delta x}$  go to 0 as  $\Delta x \rightarrow 0$ , we assume  $|1 - 6cfl + 18cfl^2| < 1$ , i.e.  $cfl < \frac{1}{3}$ . Then

$$\tilde{u}_{j-\frac{1}{4}} - U(x_{j-\frac{1}{4}}, t) = e^{-i\bar{t}} \left( \frac{\xi^2}{24} - \frac{\xi^2}{6} icfl^2 \bar{t} - i \frac{\xi^3}{576} - \frac{\xi^3}{72} \bar{t} - \frac{\xi^3}{24} cfl^2 \bar{t} + \frac{\xi^3}{8} cfl^3 \bar{t} + O(\xi^4) \right).$$

Thus

$$\begin{aligned} \|e_{-\frac{1}{4}}\|_\infty &= \max_{1 \leq j \leq N} |\tilde{u}_{j-\frac{1}{4}} - U(x_{j-\frac{1}{4}}, t)| \\ &= \left| \frac{1}{24} \sqrt{1 + 16cfl^4 \bar{t}^2} \xi^2 - \frac{(2\bar{t} + 7cfl^2 \bar{t} - 18cfl^3 \bar{t}) \xi^3}{144 \sqrt{1 + 16cfl^4 \bar{t}^2}} \right| + O(\xi^4). \end{aligned} \tag{5.5}$$

We keep the same notations here as in the semi-discrete case. Similarly,

$$\|e_{+\frac{1}{4}}\|_\infty = \frac{1}{24} \sqrt{1 + 16cfl^4 \bar{t}^2} \xi^2 + \frac{(2\bar{t} + 7cfl^2 \bar{t} - 18cfl^3 \bar{t}) \xi^3}{144 \sqrt{1 + 16cfl^4 \bar{t}^2}} + O(\xi^4) \tag{5.6}$$

and

$$\begin{aligned} e_1 &= \max \{ \|e_{-\frac{1}{4}}\|_\infty, \|e_{+\frac{1}{4}}\|_\infty \} \\ &= \frac{1}{24} \sqrt{1 + 16cfl^4 \bar{t}^2} \xi^2 + \frac{(2\bar{t} + 7cfl^2 \bar{t} - 18cfl^3 \bar{t}) \xi^3}{144 \sqrt{1 + 16cfl^4 \bar{t}^2}} + O(\xi^4). \end{aligned} \tag{5.7}$$

Since it takes a minimum of two points per wavelength to uniquely specify a wave, the largest wave number that can be represented on the  $N$  cells (reminder: two points are used for each cell) is  $\omega = \frac{2\pi}{\Delta x} = N$ . Therefore, we consider simple waves with  $0 < \omega \leq N$ . If  $\omega$  is much less than  $N$  in magnitude, then there are many grid-points per wavelength, and the solution is well resolved. In this case,  $\xi$  is a small number, and we can neglect  $O(\xi^3)$  and obtain

$$e_1 \simeq \frac{1}{24} \sqrt{1 + 16cfl^4 \bar{t}^2} \xi^2. \tag{5.8}$$

If  $\xi$  is large, corresponding to fewer gridpoints per wavelength in the solution, then the  $P^1$  solution is not a good approximation of the exact solution and approximation polynomials of degree  $> 1$  are required.

Similarly, when using RK (3,3) time discretization, the error estimates under the assumption  $cfl < 0.418$  are

$$\|e_{-\frac{1}{4}}\|_\infty = \left| \frac{\xi^2}{24} - \frac{\xi^3}{72} \bar{t} (1 + 3cfl^3) \right| + O(\xi^4), \tag{5.9}$$

$$\|e_{+\frac{1}{4}}\|_\infty = \frac{\xi^2}{24} + \frac{\xi^3}{72} \bar{t} (1 + 3cfl^3) + O(\xi^4). \tag{5.10}$$

At  $\bar{t} = O(\frac{1}{\xi})$ ,

$$e_1 \simeq \frac{\xi^2}{24} + \frac{\xi^3}{72} \bar{t} (1 + 3cfl^3). \tag{5.11}$$

The necessary number of points per wavelength required to ensure a specific error  $\varepsilon$  can be obtained by rewriting (5.8) and (5.11) in terms of  $M_1$  and  $q$  and setting  $e_1 \leq \varepsilon$ .

### 5.2. The case of $P^2$

For  $k = 2$  and  $k = 3$ , the analysis procedure is the same.

In this subsection, we present the results of fully discretized error estimates when piecewise  $P^2$  polynomials are used.

When using RK (3,3) time discretization, under the assumption  $cfl < 0.327$ , we have

$$\|e_{-\frac{1}{3}}\|_\infty = \frac{1}{1296} \sqrt{1 + \frac{7222932}{3125} cfl^6 \bar{t}^2} \xi^3 + O(\xi^4), \tag{5.12}$$

$$\|e_0\|_\infty = \frac{1}{240} \sqrt{1 + 100cfl^6 \bar{t}^2} \xi^3 + O(\xi^4), \tag{5.13}$$

$$\|e_{+\frac{1}{3}}\|_\infty = \frac{23}{6480} \sqrt{1 + \frac{72900}{529} cfl^6 \bar{t}^2} \xi^3 + O(\xi^4). \tag{5.14}$$

Thus,

$$\begin{aligned} e_2 &= \max \{ \|e_{-\frac{1}{3}}\|_\infty, \|e_0\|_\infty, \|e_{+\frac{1}{3}}\|_\infty \} \\ &\simeq \frac{1}{240} \sqrt{1 + 100cfl^6 \bar{t}^2} \xi^3. \end{aligned} \tag{5.15}$$

When using RK (4,4) time discretization, under the assumption  $cfl < 0.351$ , we have

$$\|e_{-\frac{1}{3}}\|_\infty = \frac{1}{1296} \xi^3 + \frac{\bar{t}}{120} cfl^4 \xi^4 + O(\xi^5), \tag{5.16}$$

$$\|e_0\|_\infty = \frac{1}{240} \xi^3 + \frac{\bar{t}}{120} cfl^4 \xi^4 + O(\xi^5), \tag{5.17}$$

$$\|e_{+\frac{1}{3}}\|_\infty = \left| \frac{23}{6480} \xi^3 - \frac{\bar{t}}{120} cfl^4 \xi^4 \right| + O(\xi^5). \tag{5.18}$$

At  $\bar{t} = O(\frac{1}{\xi})$ ,

$$e_2 \simeq \frac{1}{240} \xi^3 + \frac{\bar{t}}{120} cfl^4 \xi^4. \tag{5.19}$$

While at  $\bar{t} = O(\frac{1}{\xi^2})$ , we need more terms of the Taylor series to approximate  $e_2$ . In this case,

$$\begin{aligned} e_2 \simeq & |0.0041666666666667 \xi^3 + 0.0083333333333333 cfl^4 \xi^4 \bar{t} \\ & - 0.0003201517489712 \xi^5 + \xi^6 (-6.0626102292768959 \times 10^{-6} \bar{t} \\ & - 0.0000680298353909 cfl^4 \bar{t} + 0.0008873456790123 cfl^5 \bar{t} \\ & - 0.0029761904761905 cfl^6 \bar{t}) + \xi^7 (-0.00013365952729388 \\ & + 2.3148148148148 \times 10^{-6} \bar{t}^2 - 0.0000354938271605 cfl^4 \bar{t}^2 \\ & + 0.0002314814814815 cfl^5 \bar{t}^2 + 0.0001360596707819 cfl^8 \bar{t}^2 \\ & - 0.0017746913580247 cfl^9 \bar{t}^2 + 0.005787037037037 cfl^{10} \bar{t}^2)|. \end{aligned} \tag{5.20}$$

The necessary number of points per wavelength required to ensure a specific error  $\varepsilon$  can be obtained by rewriting (5.15), (5.19) and (5.20) in terms of  $M_2$  and  $q$  and setting  $e_2 \leq \varepsilon$ .

5.3. The case of  $P^3$

For the cases  $k = 1$  and  $k = 2$ , the cfl condition is consistent with the CFL<sub>L2</sub> table in [24]. However, for  $k = 3$ , we cannot get the cfl condition using the same procedure by Taylor expansion and Mathematica due to limited memory. In this subsection, we provide the error estimates based on a fixed cfl = 0.1.

When using RK (4,4) time discretization, we have

$$\|e_{\frac{3}{8}}\|_{\infty} = \zeta^4 \sqrt{3.2541560538021135 \times 10^{-8} + 6.944444444444444 \times 10^{-13} \bar{t}^2 + O(\zeta^5)},$$

$$\|e_{\frac{1}{8}}\|_{\infty} = \zeta^4 \sqrt{1.3128715187393769 \times 10^{-9} + 6.944444444444444 \times 10^{-13} \bar{t}^2 + O(\zeta^5)},$$

$$\|e_{\frac{5}{8}}\|_{\infty} = \zeta^4 \sqrt{1.3227188998669514 \times 10^{-7} + 6.944444444444444 \times 10^{-13} \bar{t}^2 + O(\zeta^5)},$$

$$\|e_{\frac{7}{8}}\|_{\infty} = \zeta^4 \sqrt{9.3484606662364834 \times 10^{-9} + 6.944444444444444 \times 10^{-13} \bar{t}^2 + O(\zeta^5)}.$$

And

$$e_3 \simeq \zeta^4 \sqrt{1.3227188998669514 \times 10^{-7} + 6.944444444444444 \times 10^{-13} \bar{t}^2}. \tag{5.21}$$

When using RK (5,5) time discretization, we have

$$\|e_{\frac{3}{8}}\|_{\infty} = 0.0001803927951389 \zeta^4 + 1.388888888888889 \times 10^{-8} \bar{t} \zeta^5 + O(\zeta^6), \tag{5.22}$$

$$\|e_{\frac{1}{8}}\|_{\infty} = 0.0000362335689484 \zeta^4 + 1.388888888888889 \times 10^{-8} \bar{t} \zeta^5 + O(\zeta^6), \tag{5.23}$$

$$\|e_{\frac{5}{8}}\|_{\infty} = 0.0003636920262897 \zeta^4 + 1.388888888888889 \times 10^{-8} \bar{t} \zeta^5 + O(\zeta^6), \tag{5.24}$$

$$\|e_{\frac{7}{8}}\|_{\infty} = 0.0000966874379960 \zeta^4 + 1.388888888888889 \times 10^{-8} \bar{t} \zeta^5 + O(\zeta^6). \tag{5.25}$$

At  $\bar{t} = O(\frac{1}{\zeta^2})$ ,

$$e_3 \simeq 0.0003636920262897 \zeta^4 + 1.388888888888889 \times 10^{-8} \bar{t} \zeta^5. \tag{5.26}$$

The necessary number of points per wavelength required to ensure a specific error  $\varepsilon$  can be obtained by rewriting (5.21) and (5.26) in terms of  $M_3$  and  $q$  and setting  $e_3 \leq \varepsilon$ .

Table 5.1 shows the  $M_k$  as a function of  $q$  (we only present the leading term here), derived from the error estimates in each subsection. These estimates is computed at  $\bar{t} = O(\frac{1}{\zeta^2})$ . Here we fix cfl = 0.3 for  $k = 1$ , cfl = 0.2 for  $k = 2$  and cfl = 0.1 for  $k = 3$ .

So far, in every case, we have expressed  $e_k$  as a function of  $M_k$  and  $q$ . Now the work per wavelength to obtain the error  $e_k$  when integrating to time  $t$  using RK ( $p,p$ ) is given by

Table 5.1

Leading term of the lower bound of  $M_k$  as a function of  $q$ .

RK ( $p,p$ )	$M_1$		$M_2$		$M_3$	
	RK (2,2)	RK (3,3)	RK (3,3)	RK (4,4)	RK (4,4)	RK (5,5)
$\varepsilon = 0.1$	$12q^{\frac{1}{2}}$	$12q^{\frac{1}{2}}$	$5q^{\frac{1}{2}}$	$3q^{\frac{1}{2}}$	$2q^{\frac{1}{2}}$	$2q^{\frac{1}{2}}$
$\varepsilon = 0.01$	$39q^{\frac{1}{2}}$	$26q^{\frac{1}{2}}$	$11q^{\frac{1}{2}}$	$8q^{\frac{1}{2}}$	$4q^{\frac{1}{2}}$	$2q^{\frac{1}{2}}$
$\varepsilon = 0.001$	$122q^{\frac{1}{2}}$	$57q^{\frac{1}{2}}$	$24q^{\frac{1}{2}}$	$10q^{\frac{1}{2}}$	$8q^{\frac{1}{2}}$	$4q^{\frac{1}{2}}$

$$W_k = 2(k + 1) \times M_k \times \frac{t}{\Delta t} \times p,$$

which is a product of the number of operations per mesh point per time step  $2k + 1$ , the number of points per wavelength  $M_k = \frac{2\pi(k+1)}{\omega\Delta x}$ , the total number of time steps  $\frac{t}{\Delta t}$  and the number of stages per time step  $p$ . Using  $\omega at = 2\pi q$  and  $cfl = a \frac{\Delta t}{\Delta x}$ , we obtain

$$\begin{aligned} W_k &= 2(k + 1)M_k p \frac{t}{\Delta t} = 2(k + 1)M_k p \frac{2\pi q}{\omega a \Delta t} = 2(k + 1)M_k p \frac{2\pi q}{\omega \Delta x cfl} \\ &= 2(k + 1)M_k p \frac{q}{cfl} \frac{2\pi}{\omega \Delta x} = 2(k + 1)M_k p \frac{q}{cfl} \frac{M_k}{k + 1} = \frac{2}{cfl} p q M_k^2. \end{aligned}$$

6. Numerical results

In this section, we provide numerical experiments to demonstrate the predicted results presented in the previous sections.

To verify the predicted results for the semi-discrete scheme, we adopt SSPRK (9,9) [26] to make the temporal error negligible compared to the spatial error. This time discretization method for solving  $du/dt = Lu$ , where  $L$  is a spatial discretization operator (for this SSP method to be ninth order,  $L$  needs to be linear) is defined as follows:

$$u^{(i)} = u^{(i-1)} + \Delta t Lu^{(i-1)}, \quad i = 1, \dots, 8,$$

$$u^{(9)} = \sum_{k=0}^7 \alpha_{9,k} u^{(k)} + \alpha_{9,8} (u^{(8)} + \Delta t Lu^{(8)}),$$

Table 6.1

When using  $P^k$  polynomials on a uniform mesh of  $\bar{N}$  cells,  $\bar{t} = 1$ .

$N$	Numerical results		Predicted by analysis	
$k = 1$	$e_1$	Order	$e_1$	Order
20	4.4639E-03		4.5430E-03	
40	1.0763E-03	2.05	1.0819E-03	2.07
80	2.6333E-04	2.03	2.6375E-04	2.04
160	6.5072E-05	2.02	6.5096E-05	2.02
$k = 2$	$e_2$	Order	$e_2$	Order
20	1.2796E-04		1.2825E-04	
40	1.6139E-05	2.99	1.6119E-05	2.99
80	2.0179E-06	3.00	2.0177E-06	3.00
160	2.5231E-07	3.00	2.5230E-07	3.00
$k = 3$	$e_3$	Order	$e_3$	Order
20	3.6972E-06		3.5497E-06	
40	2.2928E-07	4.01	2.2153E-07	4.00
80	1.3858E-08	4.05	1.3840E-08	4.00
160	8.6484E-10	4.00	8.6494E-10	4.00

Table 6.2

When using  $P^k$  polynomials on a uniform mesh of  $\bar{N}$  cells,  $\bar{t} = 100$ .

$N$	Numerical results		Predicted by analysis	
$k = 1$	$e_1$	Order	$e_1$	Order
20	4.5526E-02		4.7177E-02	
40	6.3632E-03	2.84	6.4111E-03	2.88
80	9.2878E-04	2.78	9.2990E-04	2.79
160	1.4831E-04	2.65	1.4837E-04	2.65
$k = 2$	$e_2$	Order	$e_2$	Order
20	1.3370E-04		1.3463E-04	
40	1.6120E-05	3.05	1.6164E-05	3.06
80	2.0172E-06	3.00	2.0180E-06	3.00
160	2.5226E-07	3.00	2.5230E-07	3.00
$k = 3$	$e_3$	Order	$e_3$	Order
20	3.5443E-06		3.5570E-06	
40	2.2147E-07	4.00	2.2148E-07	4.01
80	1.3831E-08	4.00	1.3838E-08	4.00
160	8.6229E-10	4.00	8.6490E-10	4.00

**Table 6.3**  
When using  $P^k$  polynomials on a uniform mesh of  $\bar{N}$  cells,  $\bar{t} = 1000$ .

N	Numerical results		Predicted by analysis	
	$e_1$	Order	$e_1$	Order
$k = 1$				
20	3.5039E-01		4.3476E-01	
40	5.3261E-02	2.72	5.4858E-02	2.99
80	6.9551E-03	2.94	6.9858E-03	2.97
160	9.0479E-04	2.94	9.0535E-04	2.95
$k = 2$				
20	4.4844E-04		8.2153E-04	
40	2.0799E-05	4.43	2.1489E-05	5.26
80	2.0575E-06	3.34	2.0589E-06	3.38
160	2.5111E-07	3.03	2.5261E-07	3.03
$k = 3$				
20	3.7047E-06		3.7487E-06	
40	2.2252E-07	4.06	2.2298E-07	4.07
80	1.3902E-08	4.00	1.3850E-08	4.01
160	8.6496E-10	4.01	8.6499E-10	4.00

where

$$\alpha_{m,0} = \frac{16687}{45360}, \quad \alpha_{m,0} = \frac{2119}{5760}, \quad \alpha_{m,2} = \frac{103}{560},$$

$$\alpha_{m,3} = \frac{53}{864}, \quad \alpha_{m,4} = \frac{11}{720}, \quad \alpha_{m,5} = \frac{1}{320},$$

$$\alpha_{m,6} = \frac{1}{2160}, \quad \alpha_{m,7} = \frac{1}{10080}, \quad \alpha_{m,8} = \frac{1}{362880}.$$

Uniform meshes are used in the calculation and the CFL condition  $cfl = a \frac{\Delta x}{\Delta t}$  is chosen from the table in [24].

Tables 6.1, 6.2, 6.3 list the error between DG solution and exact solution for fixed  $\bar{t}$  with different cell size  $\bar{N}$ , where  $\bar{N} = \frac{N}{\Delta x}$ . The numerical results are computed using  $P^k$  polynomials and RK (9,9) time discretization. The predicted results are computed using the formulas derived in Section 3. The predicted errors agree with the computed results very well. These tables also show that the orders of the errors are different at different final time  $\bar{t}$ . This is because the higher order terms of the error dominate for large  $\bar{t}$ .

Figs. 6.1, 6.2, 6.3 show the time evolution of the  $L^\infty$  error and  $e_k$  error when using  $P^k$  polynomials with three different time discretization methods. One is the same order as the spatial error, another one is one order higher than the spatial error and the last one is the RK (9,9) which makes the temporal error negligible comparing with the spatial error. The numerical  $L^\infty$  error is computed by taking a uniform partition of each element with 20 points. These figures show that the time discretization method needs to be at least one order higher than the DG method, in order to get the same result as the semi-discrete case. The order of the RK method higher than  $k + 1$  makes little difference when the DG method is using  $P^k$  polynomials. Also, the figures demonstrate that the predicted errors in general agree with the computed results very well.

Tables 6.4, 6.5, 6.6 list the numerical errors and their orders at Radau points for different final time  $\bar{t}$ . These tables verify the results derived in Section 4: the errors at the downwind point of

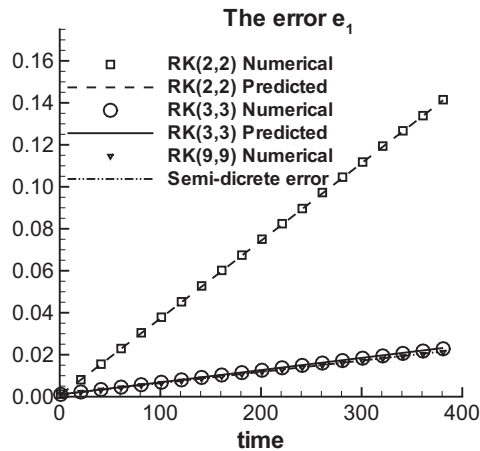
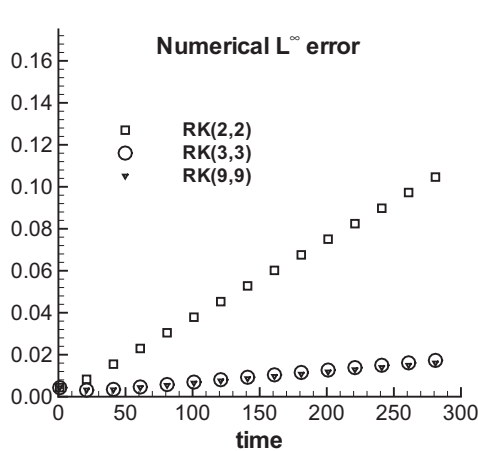


**Fig. 6.1.** Time evolution of  $L^\infty$  error (left) and  $e_1$  error (right) for  $P^1$  DG solution with  $\bar{N} = 40$ ,  $cfl = 0.3$ .

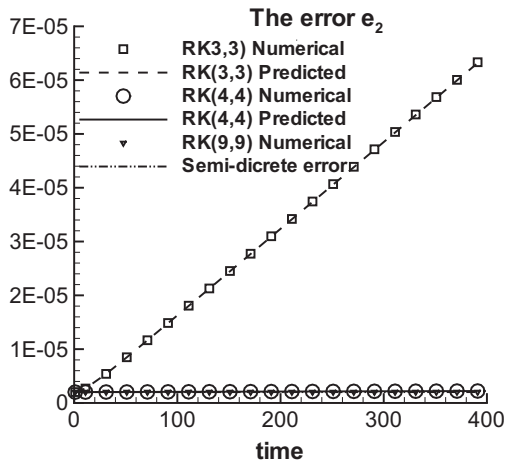
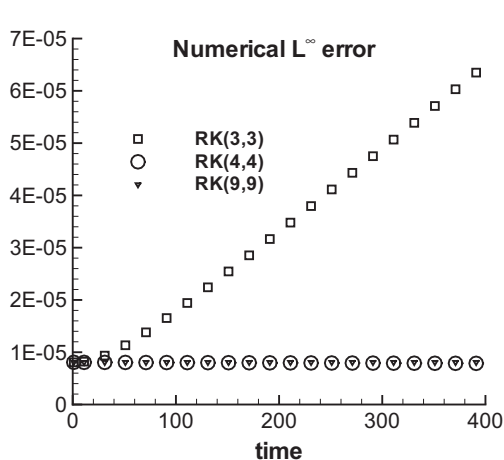


**Fig. 6.2.** Time evolution of  $L^\infty$  error (left) and  $e_2$  error (right) for  $P^2$  DG solution with  $\bar{N} = 80$ ,  $cfl = 0.2$ .

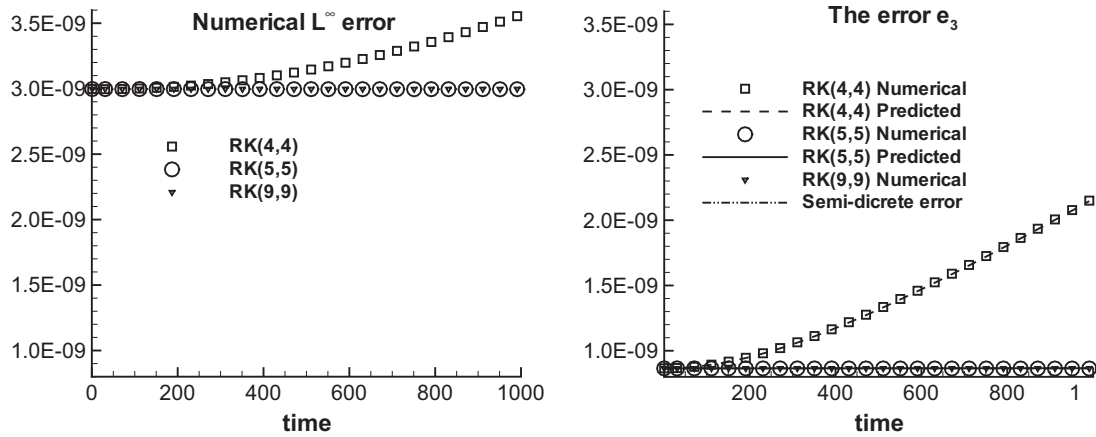


Fig. 6.3. Time evolution of  $L^\infty$  error (left) and  $e_3$  error (right) for  $P^3$  DG solution with  $\bar{N} = 160$ ,  $cfl = 0.1$ .

Table 6.4 Error at Radau points using  $P^1$  DG and RK (9,9) on a uniform mesh of  $\bar{N}$  cells.

	$\bar{N}$	$\bar{t} = 1$		$\bar{t} = 10$		$\bar{t} = 100$	
		Error	Order	Error	Order	Error	Order
$\ e_{r_0}\ _\infty$	20	4.75E-04		4.25E-03		4.17E-02	
	40	5.91E-05	3.01	5.37E-04	2.98	5.36E-03	2.96
	80	7.38E-06	3.00	6.73E-05	3.00	6.72E-04	3.00
	160	9.22E-07	3.00	8.42E-06	3.00	8.41E-05	3.00
$\ e_{\frac{1}{2}}^-\ _\infty$	20	6.97E-04		4.28E-03		4.18E-02	
	40	8.87E-05	2.97	5.39E-04	2.99	5.35E-03	2.97
	80	1.12E-05	2.99	6.77E-05	2.99	6.72E-04	2.99
	160	1.40E-06	3.00	8.48E-06	3.00	8.41E-05	3.00

Table 6.5 Error at Radau points using  $P^2$  DG and RK (9,9) on a uniform mesh of  $\bar{N}$  cells.

	$\bar{N}$	$\bar{t} = 1$		$\bar{t} = 10$		$\bar{t} = 100$	
		Error	Order	Error	Order	Error	Order
$\max_{0 \leq i \leq 1} \{\ e_{r_i}\ _\infty\}$	20	1.05E-05		1.23E-05		4.97E-05	
	40	6.73E-07	3.96	6.37E-07	4.27	1.83E-06	4.76
	80	4.25E-08	3.98	3.88E-08	4.07	7.30E-08	4.65
	160	2.67E-09	3.99	2.56E-09	3.92	3.27E-09	4.48
$\ e_{\frac{1}{2}}^-\ _\infty$	20	1.09E-06		4.34E-06		4.23E-05	
	40	3.44E-08	4.98	1.36E-07	4.99	1.33E-06	5.00
	80	1.08E-09	5.00	4.26E-09	5.00	4.15E-08	5.00
	160	3.37E-11	5.00	1.33E-10	5.00	1.30E-09	5.00

Table 6.6 Error at Radau points using  $P^3$  DG and RK (9,9) on a uniform mesh of  $\bar{N}$  cells.

	$\bar{N}$	$\bar{t} = 1$		$\bar{t} = 10$		$\bar{t} = 100$	
		Error	Order	Error	Order	Error	Order
$\max_{0 \leq i \leq 2} \ e_{r_i}\ _\infty$	20	1.64E-07		1.46E-07		1.48E-07	
	40	4.70E-09	5.12	4.60E-09	4.99	4.60E-09	5.01
	80	1.44E-10	5.02	1.44E-10	5.00	1.44E-10	5.00
	160	4.50E-12	5.00	4.50E-12	5.00	4.50E-12	5.00
$\ e_{\frac{1}{2}}^-\ _\infty$	20	1.86E-08		2.24E-09		2.13E-08	
	40	2.12E-10	6.45	1.76E-11	6.99	1.67E-10	7.00
	80	5.09E-13	8.70	1.38E-13	7.00	1.31E-12	7.00
	160	3.75E-16	10.41	1.08E-15	7.00	1.02E-14	7.00

each element are superconvergent of order  $2k + 1$  and at other Radau points are superconvergent of order  $k + 2$  when using piecewise  $P^k$  polynomials. These tables also show the relation between the error and  $\bar{t}$ : for  $k = 1$ , errors are proportional to  $\bar{t}$  while

for  $k = 2, 3$ , the leading terms of the errors do not depend on  $\bar{t}$ , thus the errors are almost the same for  $\bar{t}$  under  $O\left(\frac{1}{\bar{t}}\right)$ . We have also tested the  $P^2$  case at final time  $\bar{t} = 500$ , the error  $\max_{0 \leq i \leq 1} \{\|e_{r_i}\|_\infty\}$

achieves fifth order. This is because as  $\bar{t}$  increases to 500, the fifth order term dominates. This verifies the fact that during different time intervals, the dominant terms are different.

We have also used a non-uniform mesh which is 60% random perturbation of the uniform mesh. For example, the right end of the cell  $I_j$  is now  $x_{j+\frac{1}{2}} + 60\%(r_{j+\frac{1}{2}} - 0.5)\Delta x$ , where  $x_{j+\frac{1}{2}}, \Delta x$  are taking

**Table 6.7**  
Error at Radau points using  $P^1$  DG and RK (9,9) on a random mesh of  $\bar{N}$  cells.

	$\bar{N}$	$\bar{t} = 1$		$\bar{t} = 10$		$\bar{t} = 100$	
		Error	Order	Error	Order	Error	Order
$\ e_{r_0}\ _\infty$	20	1.82E-03		6.73E-03		6.33E-02	
	40	2.39E-04	2.93	7.68E-04	3.13	7.50E-03	3.08
	80	3.23E-05	2.89	9.05E-05	3.08	8.87E-04	3.08
	160	3.11E-06	3.37	1.22E-05	2.89	1.20E-04	2.89
	320	4.98E-07	2.64	1.49E-06	3.03	1.42E-05	3.08
$\ e_{+\frac{1}{2}}^-\ _\infty$	20	1.19E-03		6.81E-03		6.34E-02	
	40	1.50E-04	2.98	7.80E-04	3.13	7.51E-03	3.08
	80	2.27E-05	2.72	8.96E-05	3.12	8.87E-04	3.08
	160	2.36E-06	3.27	1.22E-05	2.88	1.20E-04	2.89
	320	3.51E-07	2.75	1.43E-06	3.09	1.42E-05	3.08

**Table 6.8**  
Error at Radau points using  $P^2$  DG and RK (9,9) on a random mesh of  $\bar{N}$  cells.

	$\bar{N}$	$\bar{t} = 1$		$\bar{t} = 10$		$\bar{t} = 100$	
		Error	Order	Error	Order	Error	Order
$\ e_{r_0}\ _\infty$	20	3.20E-05		3.14E-05		1.31E-04	
	40	2.63E-06	3.61	2.58E-06	3.61	4.63E-06	4.82
	80	1.55E-07	4.08	1.99E-07	3.70	2.11E-07	4.45
	160	1.32E-08	3.56	1.37E-08	3.86	1.11E-08	4.25
	320	7.70E-10	4.10	7.85E-10	4.12	7.25E-10	3.94
$\ e_{+\frac{1}{2}}^-\ _\infty$	20	1.81E-05		1.39E-05		9.31E-05	
	40	4.87E-07	5.21	5.20E-07	4.74	2.81E-06	5.05
	80	6.06E-08	3.01	3.66E-08	3.83	9.28E-08	4.92
	160	2.34E-09	4.69	1.25E-09	4.87	2.74E-09	5.08
	320	1.33E-10	4.14	6.55E-11	4.26	1.01E-10	4.76

**Table 6.9**  
Error at Radau points using  $P^3$  DG and RK (9,9) on a random mesh of  $\bar{N}$  cells.

	$\bar{N}$	$\bar{t} = 1$		$\bar{t} = 10$		$\bar{t} = 100$	
		Error	Order	Error	Order	Error	Order
$\ e_{r_0}\ _\infty$	20	3.90E-07		4.16E-07		4.71E-07	
	40	4.73E-08	3.04	3.55E-08	3.55	3.74E-08	3.65
	80	1.10E-09	5.43	8.65E-10	5.36	1.04E-09	5.17
	160	2.71E-11	5.34	3.18E-11	4.76	2.94E-11	5.14
	320	1.25E-12	4.44	1.43E-12	4.47	1.40E-12	4.39
$\ e_{+\frac{1}{2}}^-\ _\infty$	20	2.29E-07		2.71E-08		4.51E-08	
	40	1.80E-08	3.67	8.42E-09	1.69	3.91E-09	3.53
	80	2.97E-10	5.92	1.16E-10	6.19	4.84E-11	6.34
	160	8.42E-12	5.14	3.56E-12	5.02	1.25E-12	5.27
	320	2.49E-13	5.08	1.05E-13	5.08	4.71E-14	4.73

**Table 6.10**  
Necessary number of points per wavelength for  $e_k \leq \varepsilon$  when time period  $q = 1$ .

RKDG ( $p, k + 1$ )	$\varepsilon = 0.1$		$\varepsilon = 0.01$		$\varepsilon = 0.001$	
	Numerical	Predicted	Numerical	Predicted	Numerical	Predicted
RKDG (2,2)	15.02	14.63	42.87	42.47	130.06	129.81
RKDG (3,2)	13.43	14.09	34.32	34.62	92.60	92.73
RKDG (9,2)	13.14	13.82	33.83	34.14	91.86	91.99
RKDG (3,3)	8.00	6.78	15.74	14.62	31.69	31.49
RKDG (4,3)	7.61	6.66	14.37	14.20	30.17	30.46
RKDG (9,3)	7.63	6.53	14.46	14.08	30.00	30.33
RKDG (4,4)	6.16	6.17	11.10	10.98	19.25	19.52
RKDG (5,4)	6.16	6.17	11.10	10.98	19.24	19.52
RKDG (9,4)	6.16	6.17	11.10	10.98	19.24	19.52

**Table 6.11**  
Necessary number of points per wavelength for  $e_k \leq \varepsilon$  when time period  $q = 10$ .

RKDG ( $p, k + 1$ )	$\varepsilon = 0.1$		$\varepsilon = 0.01$		$\varepsilon = 0.001$	
	Numerical	Predicted	Numerical	Predicted	Numerical	Predicted
RKDG (2,2)	39.46	38.60	122.60	122.06	386.36	385.97
RKDG (3,2)	26.74	27.38	60.85	61.03	140.86	140.93
RKDG (9,2)	26.08	26.72	59.48	59.67	138.16	138.23
RKDG (3,3)	13.47	11.27	26.07	24.27	53.43	52.30
RKDG (4,3)	11.38	13.58	18.83	19.86	32.85	33.11
RKDG (9,3)	11.51	13.53	18.94	19.64	32.47	32.32
RKDG (4,4)	8.00	6.19	12.65	11.00	20.45	19.57
RKDG (5,4)	8.00	6.19	12.64	10.99	20.35	19.53
RKDG (9,4)	8.00	8.70	12.64	12.65	20.36	20.35

**Table 6.12**  
When time period  $q = 1$ .

Type of scheme	Order	Multiplies per meshpoint	Stages per timestep	$W_k$		
				$\varepsilon = 0.1$	$\varepsilon = 0.01$	$\varepsilon = 0.001$
RKDG (2,2)	2	4	2	2900	24,000	224,700
RKDG (3,2)	2	4	3	4000	24,000	172,000
RKDG (3,3)	3	6	3	1400	6400	29,800
RKDG (4,3)	3	6	4	1800	8100	37,100
RKDG (4,4)	4	8	4	3000	9600	30,500
RKDG (5,4)	4	8	5	3800	12,000	38,100

**Table 6.13**  
When time period  $q = 10$ .

Type of scheme	Order	Multiplies per meshpoint	Stages per timestep	$W_k$		
				$\varepsilon = 0.1$	$\varepsilon = 0.01$	$\varepsilon = 0.001$
RKDG (2,2)	2	4	2	201,400	1,995,300	19,891,700
RKDG (3,2)	2	4	3	149,900	745,000	3,972,500
RKDG (3,3)	3	6	3	38,100	176,800	820,400
RKDG (4,3)	3	6	4	51,800	157,800	438,600
RKDG (4,4)	4	8	4	30,600	96,900	306,300
RKDG (5,4)	4	8	5	38,300	120,800	381,500

values under the uniform mesh and  $r_{j+\frac{1}{2}}$  is a random number from the uniform distribution over the range (0,1). Tables 6.7, 6.8, 6.9 list the errors and their orders at Radau points in this case for different final time  $\bar{t}$ , when using piecewise  $P^k$  polynomials. We can see that the error at Radau points is of order around  $k + 2$ , including the downwind point. We have also tested the cases of  $P^2$  and  $P^3$  using 1% random perturbation of the uniform perturbation. The numerical results still do not show the strong superconvergence of order  $2k + 1$ .

Tables 6.10 and 6.11 list the necessary number of points per wavelength required to guarantee  $e_k \leq \varepsilon$  for various RKDG schemes and values of  $\varepsilon$ . Denote RKDG ( $p, k + 1$ ) to be the scheme using the RK ( $p, p$ ) method for time discretization and the DG method with piecewise  $P^k$  polynomials for space discretization. For these schemes with RK (9,9) method, the results of semi-discrete case are used as the predicted results. These two tables also verify our conclusions about the error estimates with different time discretization methods, which states that the RK method needs to be at least one order higher than the DG method, in order to get the same result as the semi-discrete case; and there is little difference among the RK methods of order higher than  $k + 1$  when the DG method is using piecewise  $P^k$  polynomials.

Tables 6.12 and 6.13 list the work per wavelength of the scheme RKDG ( $p, k + 1$ ),  $w_k$ , required to obtain the error  $\varepsilon$  when time period  $q = 1$  and  $q = 10$ . We should point out that we could have increased the order of the RK method used in the scheme RKDG ( $k + 2, k + 1$ ) without significantly affecting the number of points per wavelength, but the numbers of stages per timestep

would then increase considerably and so is the work per wavelength.

It is clear that even for short time period, high order methods are the most appropriate choice when accuracy is the primary consideration. When using  $P^k$  polynomials for the DG method, RK ( $k + 1, k + 1$ ) needs less work than the RK ( $k + 2, k + 2$ ) for the short time period. While for long time period, the better choice is RK ( $k + 2, k + 2$ ).

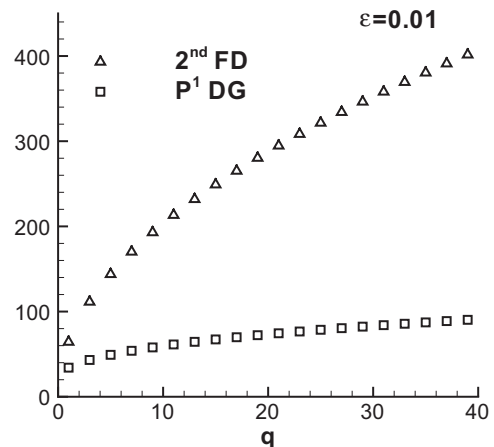


**Fig. 6.4.** Necessary points per wave for  $\|e\|_{\infty} \leq \varepsilon$ .

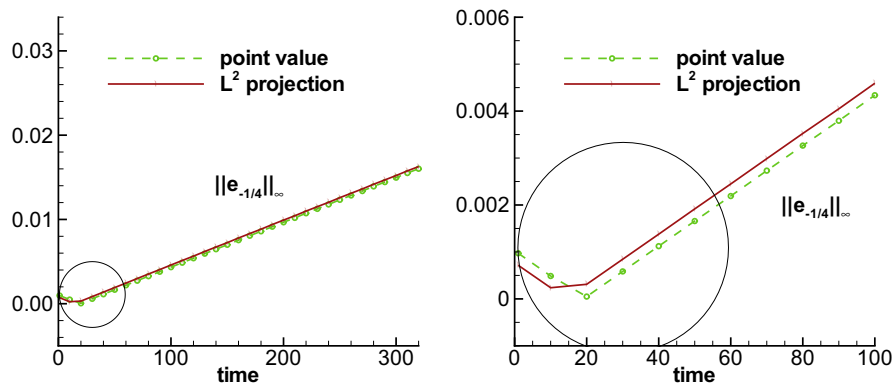


Fig. 6.5. Comparison of time evolution of the error  $\|e_{-1/4}\|_{\infty}$  with two different initial interpolations.

In Fig. 6.4, we compare the necessary number of points per wavelength required to obtain a fixed error 0.01 between two second order accurate methods. One is the DG method with  $P^1$  polynomials and the other is the second order finite difference method. It can be seen clearly that, even for a short time period, the DG method needs much less points per wavelength. Also, the necessary number of points per wavelength of the finite difference scheme grows faster with time than the RKDG method. This is because the leading term of the error for the RKDG method does not depend on  $\bar{t}$ , while the finite difference method does. This conclusion also holds for higher order schemes between the DG method and the finite difference method with the same order. In [33], Swartz and Wendroff computed the necessary number of intervals per wavelength required to obtain a fixed error for the finite element method using smooth splines as basis functions and various time discretization methods, such as the trapezoidal method and the leap-frog method. With the same order of time discretization method and space discretization method, the RKDG method requires less intervals per wavelength than the finite element method with smooth splines as basis functions in order to obtain a specified error. Moreover, the leading term of the error of this finite element method using smooth splines depends on  $\bar{t}$ . This means the necessary number of interval per wavelength for the finite element method using smooth splines also grows faster with time than the RKDG method.

**Remark.** All the numerical results and the predicted results take point value collocation as initial conditions in this paper. The usual way of taking initial conditions in a finite element method is via an  $L^2$  projection. However this does not affect the results in our paper. See Fig. 6.5.

## 7. Conclusion

In this paper, by Fourier analysis, we have derived the quantitative error estimates of the DG solutions using piecewise  $P^k$  polynomials with  $1 \leq k \leq 3$ , for solving time dependent linear wave problems. We have proved the superconvergence property of the DG solution at Radau points. The error of the DG solution is of order  $2k + 1$  superconvergence at the downwind point of each element and is of order  $k + 2$  superconvergence at other Radau points. We also provide a fully discretized error analysis with various Runge–Kutta methods. We have computed the necessary number of points per wavelength required to obtain a fixed error for several RKDG schemes. A very important implication of the discussion in this paper is that the dominant terms of the error for the RKDG schemes are different during different time intervals. This further

justifies the advantage of choosing DG methods for long time simulation of linear wave equations.

The technique of Fourier analysis discussed in this paper can be extended to the hyperbolic systems with constant coefficients. Theoretically, it can also be extended to the multidimensional case, however the algebraic manipulations may become prohibitively complicated.

## References

- [1] S. Adjerid, M. Aiffa, J. Flaherty, High-order finite element methods for singularly perturbed elliptic and parabolic problems, *SIAM J. Appl. Math.* 55 (1995) 520–543.
- [2] S. Adjerid, K. Devine, J. Flaherty, L. Krivodonova, A posteriori error estimation for discontinuous Galerkin solutions of hyperbolic problems, *Comput. Methods Appl. Mech. Engrg.* 191 (2002) 1097–1112.
- [3] S. Adjerid, A. Klausner, Superconvergence of discontinuous finite element solutions for transient convection-diffusion problems, *J. Sci. Comput.* 22–23 (2005) 5–24.
- [4] S. Adjerid, T.C. Massey, A posteriori discontinuous finite element error estimation for two-dimensional hyperbolic problems, *Comput. Methods Appl. Mech. Engrg.* 191 (2002) 5877–5897.
- [5] S. Adjerid, T.C. Massey, Superconvergence of discontinuous Galerkin solutions for a nonlinear scalar hyperbolic problem, *Comput. Methods Appl. Mech. Engrg.* 195 (2006) 3331–3346.
- [6] S. Adjerid, T. Weinhart, Discontinuous Galerkin error estimation for linear symmetric hyperbolic systems, *Comput. Methods Appl. Mech. Engrg.* 198 (2009) 3113–3129.
- [7] S. Adjerid, T. Weinhart, Discontinuous Galerkin error estimation for linear symmetrizable hyperbolic systems, *Math. Comput.* 80 (2011) 1335–1367.
- [8] M. Ainsworth, Dispersive and dissipative behaviour of high order discontinuous Galerkin finite element methods, *J. Comput. Phys.* 198 (2004) 106–130.
- [9] M. Ainsworth, P. Monk, W. Muniz, Dispersive and dissipative properties of discontinuous Galerkin finite element methods for the second-order wave equation, *J. Sci. Comput.* 27 (2006) 5–40.
- [10] M. Bakker, A note on  $C^0$  Galerkin methods for two-point boundary problems, *Numer. Math.* 38 (1982) 447–452.
- [11] M. Bakker, One-dimensional Galerkin methods and superconvergence at interior nodal points, *SIAM J. Numer. Anal.* 21 (1984) 101–110.
- [12] R. Biswas, K. Devine, J. Flaherty, Parallel adaptive finite element methods for conservation laws, *Appl. Numer. Math.* 14 (1994) 255–284.
- [13] P. Castillo, A superconvergence result for discontinuous Galerkin methods applied to elliptic problems, *Comput. Methods Appl. Mech. Engrg.* 192 (2003) 4675–4685.
- [14] F. Celiker, B. Cockburn, Superconvergence of the numerical traces for discontinuous Galerkin and hybridized methods for convection-diffusion problems in one space dimension, *Math. Comput.* 76 (2007) 67–96.
- [15] Y. Cheng, C.-W. Shu, Superconvergence and time evolution of discontinuous Galerkin finite element solutions, *J. Comput. Phys.* 227 (2008) 9612–9627.
- [16] Y. Cheng, C.-W. Shu, Superconvergence of local discontinuous Galerkin methods for one-dimensional convection-diffusion equations, *Comput. Struct.* 87 (2009) 630–641.
- [17] Y. Cheng, C.-W. Shu, Superconvergence of discontinuous Galerkin and local discontinuous Galerkin schemes for linear hyperbolic and convection-diffusion equations in one space dimension, *SIAM J. Numer. Anal.* 47 (2010) 4044–4072.
- [18] B. Cockburn, S. Hou, C.-W. Shu, TVB Runge–Kutta local projection discontinuous Galerkin finite element method for conservation laws IV: the multidimensional case, *Math. Comput.* 54 (1990) 545–581.

- [19] B. Cockburn, S.Y. Lin, C.-W. Shu, TVB Runge–Kutta local projection discontinuous Galerkin methods of scalar conservation laws III: one dimensional systems, *J. Comput. Phys.* 84 (1989) 90–113.
- [20] B. Cockburn, M. Luskin, C.-W. Shu, E. Süli, Enhanced accuracy by post-processing for finite element methods for hyperbolic equations, *Math. Comput.* 72 (2003) 577–606.
- [21] B. Cockburn, C.-W. Shu, TVB Runge–Kutta local projection discontinuous Galerkin finite element method for conservation laws II: general framework, *Math. Comput.* 52 (1989) 411–435.
- [22] B. Cockburn, C.-W. Shu, The Runge–Kutta local projection  $P^1$ -discontinuous-Galerkin method for scalar conservation laws, *Math. Model. Numer. Anal. (M<sup>2</sup>AN)* 25 (1991) 337–361.
- [23] B. Cockburn, C.-W. Shu, The Runge–Kutta discontinuous Galerkin method for conservation laws V: multidimensional systems, *J. Comput. Phys.* 141 (1998) 199–224.
- [24] B. Cockburn, C.-W. Shu, Runge–Kutta discontinuous Galerkin methods for convection-dominated problems, *J. Sci. Comput.* 16 (2001) 173–261.
- [25] J. Douglas, T. Dupont, Some superconvergence results for Galerkin methods for the approximate solution of two-point boundary value problems, in: *Topics in Numerical Analysis II, Proceedings of the Royal Irish Academy Conference Dublin, 1972*, Academic Press, 1973, pp. 89–93.
- [26] S. Gottlieb, C.-W. Shu, E. Tadmor, Strong stability preserving high order time discretization methods, *SIAM Rev.* 43 (2001) 89–112.
- [27] F.Q. Hu, H.L. Atkins, Eigensolution analysis of the discontinuous Galerkin method with nonuniform grids: I. one space dimension, *J. Comput. Phys.* 182 (2002) 516–545.
- [28] F.Q. Hu, H.L. Atkins, Two dimensional wave analysis of the discontinuous Galerkin method with non-uniform grids and boundary conditions, in: *Proceedings of the Eighth AIAA/CEAS Aeronautics Conference, Breckenridge, Colorado June 2002*, AIAA paper no. 2002-2514.
- [29] O. Karakashian, C. Makridakis, A space-time finite element method for the nonlinear Schrödinger equation: the discontinuous Galerkin method, *Math. Comput.* 67 (1998) 479–499.
- [30] H.-O. Kreiss, J. Olinger, Comparison of accurate methods for the integration of hyperbolic equations, *Tellus* 24 (1972) 199–215.
- [31] W.H. Reed, T.R. Hill, Triangular mesh methods for the neutron transport equation, Technical Report LA-UR-73-479, Los Alamos Scientific Laboratory, Los Alamos, 1973.
- [32] S.J. Sherwin, Dispersion analysis of the continuous and discontinuous Galerkin formulations, in: B. Cockburn, G. Karniadakis, C.-W. Shu (Eds.), *Discontinuous Galerkin methods: Theory, Computational and Applications*, Springer, Berlin, 2000, pp. 425–431.
- [33] B. Swartz, B. Wendroff, The relative efficiency of finite difference and finite element methods, *SIAM J. Numer. Anal.* 11 (1974) 979–993.
- [34] M. Zhang, C.-W. Shu, An analysis of three different formulations of the discontinuous Galerkin method for diffusion equations, *Math. Models Methods Appl. Sci. (M<sup>3</sup>AS)* 13 (2003) 395–413.
- [35] M. Zhang, C.-W. Shu, An analysis of and a comparison between the discontinuous Galerkin and the spectral finite volume methods, *Comput. Fluids* 34 (2005) 581–592.
- [36] M. Zhang, C.-W. Shu, Fourier analysis for discontinuous Galerkin and related methods, *Chin. Sci. Bull.* 54 (2009) 1809–1816.